

## A widely felt Tremor ( $M_L$ 3.5) of 12 April 2020 in and around NCT Delhi in the backdrop of prevailing COVID-19 pandemic lockdown: analysis and observations

Ajeet P. Pandey , G. Suresh , A.P. Singh , Anup K. Sutar & Brijesh K. Bansal

To cite this article: Ajeet P. Pandey , G. Suresh , A.P. Singh , Anup K. Sutar & Brijesh K. Bansal (2020) A widely felt Tremor ( $M_L$  3.5) of 12 April 2020 in and around NCT Delhi in the backdrop of prevailing COVID-19 pandemic lockdown: analysis and observations, Geomatics, Natural Hazards and Risk, 11:1, 1638-1652, DOI: [10.1080/19475705.2020.1810785](https://doi.org/10.1080/19475705.2020.1810785)

To link to this article: <https://doi.org/10.1080/19475705.2020.1810785>



© 2020 The Author(s). Published by Informa UK Limited, trading as Taylor & Francis Group.



Published online: 26 Aug 2020.



Submit your article to this journal [↗](#)



View related articles [↗](#)



View Crossmark data [↗](#)



# A widely felt Tremor ( $M_L$ 3.5) of 12 April 2020 in and around NCT Delhi in the backdrop of prevailing COVID-19 pandemic lockdown: analysis and observations

Ajeet P. Pandey, G. Suresh, A.P. Singh, Anup K. Sutar and Brijesh K. Bansal

National Centre for Seismology, Ministry of Earth Sciences, New Delhi, India

## ABSTRACT

An earthquake of small magnitude ( $M_L$  3.5) occurred on 12 April 2020 near the east district boundary of NCT, Delhi with maximum PGA for the event observed to be 14.13 gals. A few smaller after-shocks also occurred in the area. The estimated fault plane solution of the mainshock suggests normal faulting with some strike slip component. The focal mechanism corroborates with the NE - SW orienting lineaments mapped in the region near the epicenter. The source parameters of the event, namely, seismic moment, stress drop, corner frequency, and source radius are estimated to be  $1.15 \times 10^{14}$  N-m, 25.7 bars, 5.7 Hz and 300 m, respectively. The decay rate of acceleration with epicentral distance suggests a regression relation  $PGA = 474D^{-1.347}$ , which may be useful for understanding the ground motion in the region. A noise analyses at NDI rock and UJWA soil sites clearly suggest a significant reduction in ambient noise by  $\sim 10$  dB in the frequency band (1.0–10.0) Hz at the respective sites, during the COVID-19 lockdown situation. The reductions of the noise level improve the signal to noise ratio substantially at all the seismic stations located in the urban agglomerations, which enabled the recording of clear phases of the event and hence improved the analysis.

## ARTICLE HISTORY

Received 11 May 2020  
Accepted 23 July 2020

## KEYWORDS

Mainshock; seismic stations; source parameters; peak ground acceleration; seismic noise; lockdown

## 1. Introduction

On 12 April 2020 (Sunday), the National Capital Territory (NCT) Delhi and its neighborhood jolted with a sudden shaking caused due to a small magnitude tremor ( $M_L$  3.5), which occurred at local time 17:45:02.3 IST (12:15:02.3 UTC) in the National Capital Region (NCR) near the east district boundary of NCT Delhi. It was a time when the entire country including the NCR of Delhi was under lockdown after the unprecedented COVID-19 pandemic outburst. Although the ground motion lasted only for a few seconds, it created panic in the people and caused them to rush out of their homes. On Sunday evening, in countrywide lockdown situation, mostly

CONTACT Ajeet P. Pandey Email id: [ajeet.moes@gmail.com](mailto:ajeet.moes@gmail.com)

© 2020 The Author(s). Published by Informa UK Limited, trading as Taylor & Francis Group.

This is an Open Access article distributed under the terms of the Creative Commons Attribution License (<http://creativecommons.org/licenses/by/4.0/>), which permits unrestricted use, distribution, and reproduction in any medium, provided the original work is properly cited.

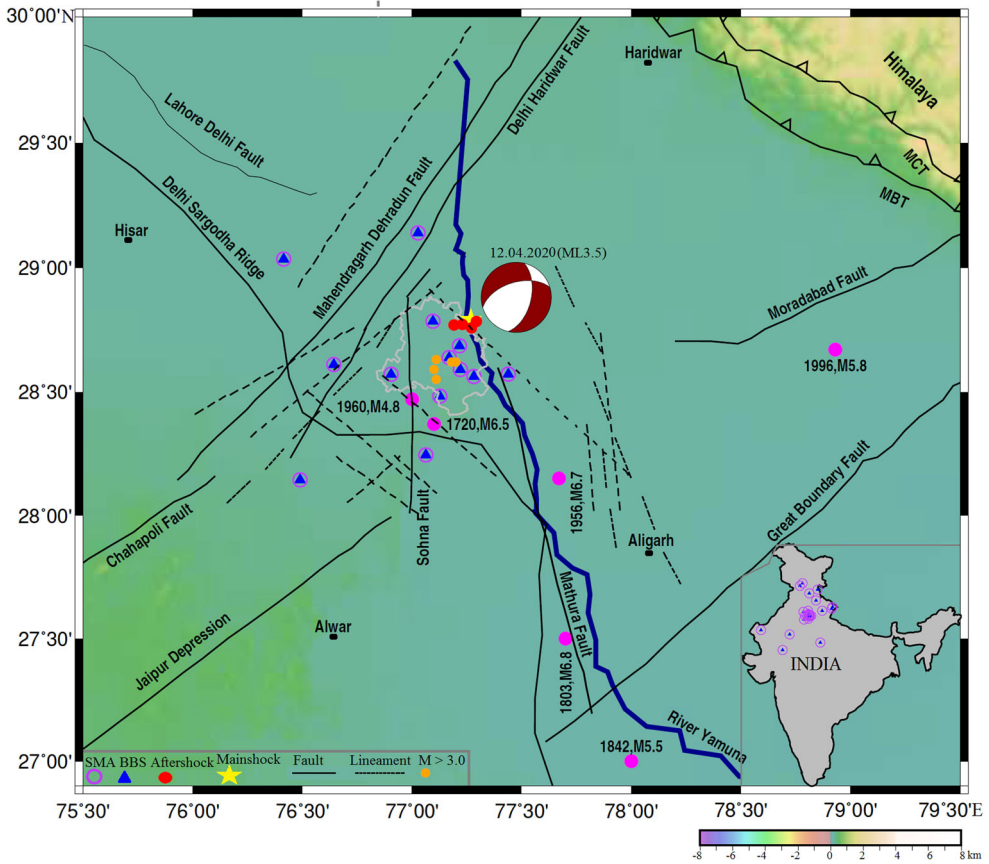


**Figure 1.** Map showing major seismotectonic features and lineaments. The recent mainshock ( $M_L 3.5$ ) of 12 April 2020 and aftershocks (12–16 April 2020) are shown by yellow star and red circles, respectively. The focal mechanism of the mainshock is shown. Significant past earthquakes are shown by pink solid circles. Earthquakes of  $M \geq 3.0$  within NCT, Delhi are shown by orange color. The curvilinear line shows the Delhi boundary. Legend and Topography scale are shown in the lower left side and at the bottom of the map, respectively. The locations of 25 seismic stations used in the analysis are depicted in the inset.

the people were confined in their houses, also primarily of multi-storeyed type, where they heard a rumbling sound on the passage of the seismic waves. No damage was reported in the region. The mainshock ( $M_L 3.5$ ) was later followed by few mild aftershocks with magnitudes  $< 3.0$ ; the events of  $M_L 1.3$ – $2.7$  occurred during 12.04.2020 to 16.04.2020. These recent Delhi earthquakes were recorded by the national network, which is operated and maintained by National Centre for Seismology (NCS), New Delhi. Evidently, the mainshock of 12 April 2020 was recorded at more than 29 seismic stations. The tremor was widely felt in the region including NCR.

**Figure 1** shows the epicentres of the mainshock and the subsequent aftershocks, which occurred during April 12–16, 2020. The NCT Delhi lies in the seismic zone IV of the seismic zoning map of India (BIS: 1893 (Part 1), 2002), which corresponds to a peak ground acceleration (PGA) equivalent to 0.24 g (i.e. 240 gals). The region has a well-known history of the felt earthquakes, both from local as well as regional sources

**Table 1.** List of historical and some significant past earthquakes of National Capital Region (NCR) Delhi.

S. N.	Date of Occurrence of Earthquakes	Epicenter		Magnitude (M)	Region
		Latitude ( $^{\circ}$ N)	Longitude ( $^{\circ}$ E)		
1	1720-07-15	28.37	77.10	6.5	Delhi
2	1803-09-01	27.50	77.70	6.8	Mathura
3	1842-01-16	27.00	78.00	5.5	Near Mathura
4	1956-10-10	28.15	77.67	6.7	Near Bulandshahar
5	1960-08-27	28.47	77.00	4.8	Delhi Cantonment – Gurugram Border
6	1996-08-15	28.67	78.93	5.8	Near Moradabad

Source: NCS earthquake catalog.

(Verma et al. 1995; Iyengar 1999). Table 1 shows a list of the historical and some significant past earthquakes in and around the Delhi region. A moderate size earthquake of 27 August 1960 was earlier located near the Delhi – Gurgaon border having magnitude M 4.8 (Table 1) but was later revised to M 6.0 (Iyengar 1999). Additionally, we mention a few more significant earthquakes like, 28 July 1994 (M4.0), 28 February 2001 (M4.0), 28 April 2001 (M3.4), 18 March 2004 (M2.6); 25 April 2007 (M4.1); 26 November 2007 (M4.1) and 07 September 2011 (M3.8) that shook the Delhi and surrounding regions. Further, about 310 tremors of  $M > 3.0$  have been reported in Delhi NCR since 1720. However, it is emphasized that no single earlier event occurred in the mainshock region for the last more than four decades (NCS, Catalog).

In the present study, we relocated the recent Delhi tremors and also analyzed the best recorded waveforms to understand the focal mechanism, source parameters, strong ground motions and their impact in the region. The results from the analyses and observations are presented in this paper. A similar analysis, however, for the aftershocks couldn't be carried out, as they were recorded at only a few seismic stations. Further, an effort is made to characterize implication of the COVID-19 lockdown silence on the ambient ground noise, which highlights the temporarily improved seismic recording due the coronavirus shutdown.

## 2. Seismotectonics of the Delhi region

A seismotectonic map of the Delhi region is shown in Figure 1. The region is located on a folded crustal ramp represented by quartzite basement rocks of the Delhi super Group, bounded between two regional faults namely, the Mahendragarh Dehradun Sub Surface Fault (MDSSF) to the west of NCT Delhi and the Great Boundary Fault (GBF) to the east. Another important structural element of the belt is the NW - SE trending Delhi Sargodha Ridge (DSR), which is flanked by the Sahaspur and Bikaner Basins to the north and southwest, respectively, and crosses the MDSSF close to Delhi. Another N-S trending fault, known as the Sohna Fault (SF), is running from Sohna to the western part of Delhi. All the tectonic features are found to be quite active and also, they are the possible causative sources of the seismicity in and around the Delhi region (e.g. Hukku 1966; Gupta and Sharda 1996; Bansal et al. 2009; Bansal and Verma 2012; Shukla et al. 2016; Singh 2020; Tripathy-Lang 2020). Moreover, the NE – SW orienting faults and lineaments mapped in the region are found to be

**Table 2.** Details of the seismic stations considered in the analysis including respective epicentral distance and azimuth from 12 April 2020 ( $M_L$  3.5) earthquake.

S. N.	Name of Station	Station Code	State / UT	Latitude ( $^{\circ}$ N)	Longitude ( $^{\circ}$ E)	Height a.m.s.l. (m)	Epicentral Distance (approx.) (km)	Azimuth
1	Ayanagar	AYA	Delhi	28.482	77.127	278	35	202
2	Lodhi Road	LDR	Delhi	28.590	77.220	209	20	192
3	Ujwa, Najafgarh	UJW	Delhi	28.570	76.904	206	45	234
4	Narela	NRL	Delhi	28.784	77.096	208	19	292
5	Kamla Nehru Ridge	NDI	Delhi	28.685	77.216	239	10	203
6	J.M.I. University	JMI	Delhi	28.562	77.282	215	23	175
7	NPL, Pusa	NPL	Delhi	28.638	77.169	222	18	209
8	Jhajjar	JHJ	Haryana	28.610	76.643	211	71	251
9	Kundal	KUD	Haryana	28.144	76.489	287	110	227
10	Rohtak	RTK	Haryana	29.034	76.414	230	99	76
11	Sohna	SON	Haryana	28.245	77.063	227	62	198
12	Ganaur	GNR	Haryana	29.139	77.027	230	49	45
13	Kalpa	KLP	Himachal Pradesh	31.547	78.260	2672	328	17
14	Shimla	SML	Himachal Pradesh	31.128	77.174	2130	262	358
15	Talwara	TLW	Himachal Pradesh	31.956	75.956	473	383	373
16	Dharamshala	DHR	Himachal Pradesh	32.248	76.307	1878	401	347
17	Ajmer	AJM	Rajasthan	26.424	74.629	497	391	226
18	Jaisalmer	JAS	Rajasthan	26.924	70.903	262	735	253
19	Udaipur	UDP	Rajasthan	24.580	73.713	586	609	218
20	Bisrakh	BIS	Uttar Pradesh	28.571	77.439	204	29	146
21	Jhansi	JHN	Uttar Pradesh	25.455	78.613	240	397	161
22	Thakurdwara	TKD	Uttar Pradesh	29.149	78.855	212	182	75
23	Dehradun	DDI	Uttarakhand	30.322	78.054	642	194	24
24	Lohaghat	LGT	Uttarakhand	29.399	80.088	1657	321	
25	Pithoragarh	PTH	Uttarakhand	29.586	80.204	1601	339	72

consistent with the nodal planes of a few past Delhi earthquakes (Singh et al. 2010). Seismically the most active regions of the Himalaya namely, the Main Central Thrust (MCT), and Main Boundary Thrust (MBT) strongly influence the seismic activity in the Delhi region and also, they are probably the liable to the genesis of the moderate damaging events (NCS Catalog; GSI 2000).

### 3. Data analysis and results

Earthquake monitoring in Delhi and surrounding regions is efficiently carried out using a state-of-the-art digital telemetered national network equipped with broadband seismographs (BBS) and Strong Motion Accelerographs (SMA) spread across the region. In the back drop of the prevailing lockdown due to the COVID crisis, the recent earthquake  $M_L$  3.5 of 12 April 2020 is an unusually well-recorded tremor in the region due to reduced ambient noise level at the recording stations. In the present study, we relocated the mainshock using well recorded data from 25 seismic stations showing clear P- and S- phases as well as improved signal to noise ratio (SNR). Figure 1 shows the location map of the field seismic stations (BBS and SMA) that were considered in the analysis. Details of the recording stations including the azimuths and epicentral distances are listed in Table 2. Apparently, nine seismic stations are within the radius of 50 km from the epicenter of the mainshock. Two stations are within the distance range 50–100 km, while three stations are located between 100 km

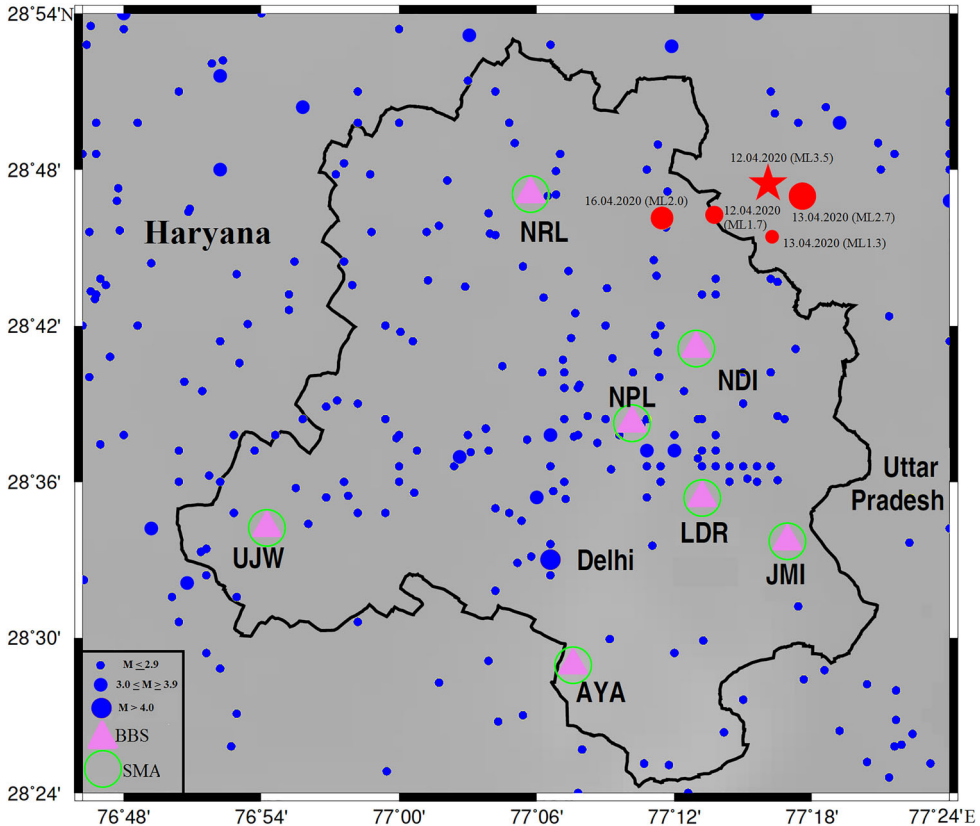


**Figure 2.** Distribution of earthquakes in and around the NCT Delhi during January 2001 - March 2020 is shown by the blue circles. The violet curvilinear line shows the Delhi boundary. The seismic stations (SMA and BBS) used in the recording recent events within NCT are depicted.

and 200 km, and the remaining stations are beyond 200 km. We mention that the BBS and SMA stations are collocated at each site. The well recorded earthquakes of the Delhi region for the last about two decades (January, 2001 – March, 2020) clearly demarcate the zones of seismic activity (Figure 2). During this period, about 733 earthquakes have been located in and around Delhi (NCS, Catalog); more than 90% events of these are of magnitude  $< 3.0$  having focal depth  $\leq 15$  km. The NCT, however, witnessed about 146 events during the period, including an event (on 25 November 2007) with maximum magnitude  $M_w$  4.1 (Singh et al. 2010).

### 3.1. Source characterization

#### 3.1.1. Earthquake location

The mainshock of 12 April 2020 is well recorded by 25 seismic stations in and around the NCT. The event was relocated using the SEISAN software package (Havskov and Ottemoller 1999), and the epicenter is estimated to be (28.791°N, 77.268°E) with rms error 0.23 s, and the focal depth is found to be  $\sim 14.5$  km. The accuracy of the location in latitude and longitude was estimated to be about  $\pm 1.0$  km

**Table 3.** Estimated focal parameters of the recent earthquakes occurred in Delhi region during 12–16 April 2020.

S. N.	Date / Origin Time (IST)	Latitude ( $^{\circ}$ N)	Longitude ( $^{\circ}$ E)	Focal Depth (km)	Error in Lat. (km)	Error in Long. (km)	Error in depth (km)	RMS (km)	Magnitude ( $M_L$ )
1.	2020-04-12 / 17:45:02.3	28.791	77.268	14.5	1.0	1.4	1.5	0.23	3.5
2.	2020-04-12 / 17:50:45.8	28.771	77.229	14.3	3.9	3.6	2.7	0.71	1.7
3.	2020-04-13 / 13:26:30.8	28.783	77.293	13.8	2.6	2.6	2.1	0.26	2.7
4.	2020-04-13 / 14:09:21.8	28.757	77.271	15.5	2.3	4.7	2.1	0.24	1.3
5.	2020-04-16 / 08:26:22.8	28.769	77.191	14.0	4.1	4.0	3.2	0.41	2.0

and  $\pm 1.4$  km respectively; however, the focal depth accuracy was about  $\pm 1.5$  km. Details of the focal parameters are listed in Table 3. An aftershock that occurred on 13 April 2020 ( $M_{2.7}$ ) was also relocated in a similar manner using well recorded data from 9 seismic stations. However, the other mild aftershocks during 13–16 April 2020 could not be relocated as they were recorded at only a few stations.

### 3.1.2. Focal mechanism

A well constrained focal mechanism of an earthquake of 25 November 2007 ( $M_{4.1}$ ) within NCT Delhi suggests strike–slip faulting with some normal component (Singh et al. 2010). Two more tremors, viz., 28 April 2001 ( $M_{3.4}$ ) and 18 March 2004 ( $M_{2.6}$ ) of NCT, also revealed a similar faulting mechanism having strike slip with some normal component (Bansal et al. 2009). In the present study, we have simulated the recent earthquake of 12 April 2020 for the fault plane solution using the ISOLA waveform inversion technique (Sokos and Zahradnik 2008). Well recorded waveform data from nine BBS stations, which were located within 100 km epicentral distance except KUDL station located at 110 km (Table 2), were used in the analysis. We mention that for three stations, namely, LDR, JMIU and GNR, although they were located within 50 km from the epicenter, the records were too noisy to be used in the analysis. The waveforms with cut-off SNR  $> 2.0$  in the frequency range of interest (0.05–15 Hz) were used in the inversion. Various available velocity models for the study region were tested for the simulation (e.g. Chun 1986; Kayal 2001; Suresh et al. 2008; Kumar et al. 2009; Mitra et al. 2011), and the model of Mitra et al. (2011) was found the most suitable to compute synthetic waveform with high correlation coefficient and DC %. The component-wise best fits between the synthetic and the recorded waveforms in the frequency band 0.06–0.1 Hz are shown in Figure 3(a). Some seismic stations as well as components of the simulated waveforms that showed negative correlation and did not match well with the observed waveforms were excluded from the analysis to get the moment tensor solution. Figure 3(b) shows the estimated fault plane solution of the 12 April 2020 event using a vertical grid search method at various trial depths, and the best solution was achieved for the correlation  $> 0.5$  and DC%  $> 70$ , which suggests normal faulting with a strike slip component. Further, the moment magnitude of the event is estimated to be  $M_w 3.5$ . Table 4 shows the fault plane solution of the 12 April 2020 mainshock, and the final beach ball is depicted in Figure 1. The nature of faulting of the current event and one of its nodal planes oriented NNE – SSW corroborate well with the results of earlier small magnitude earthquakes that occurred in NCT (Bansal et al. 2009; Singh et al. 2010). We also found a nodal plane consistent with orientation of lineaments mapped

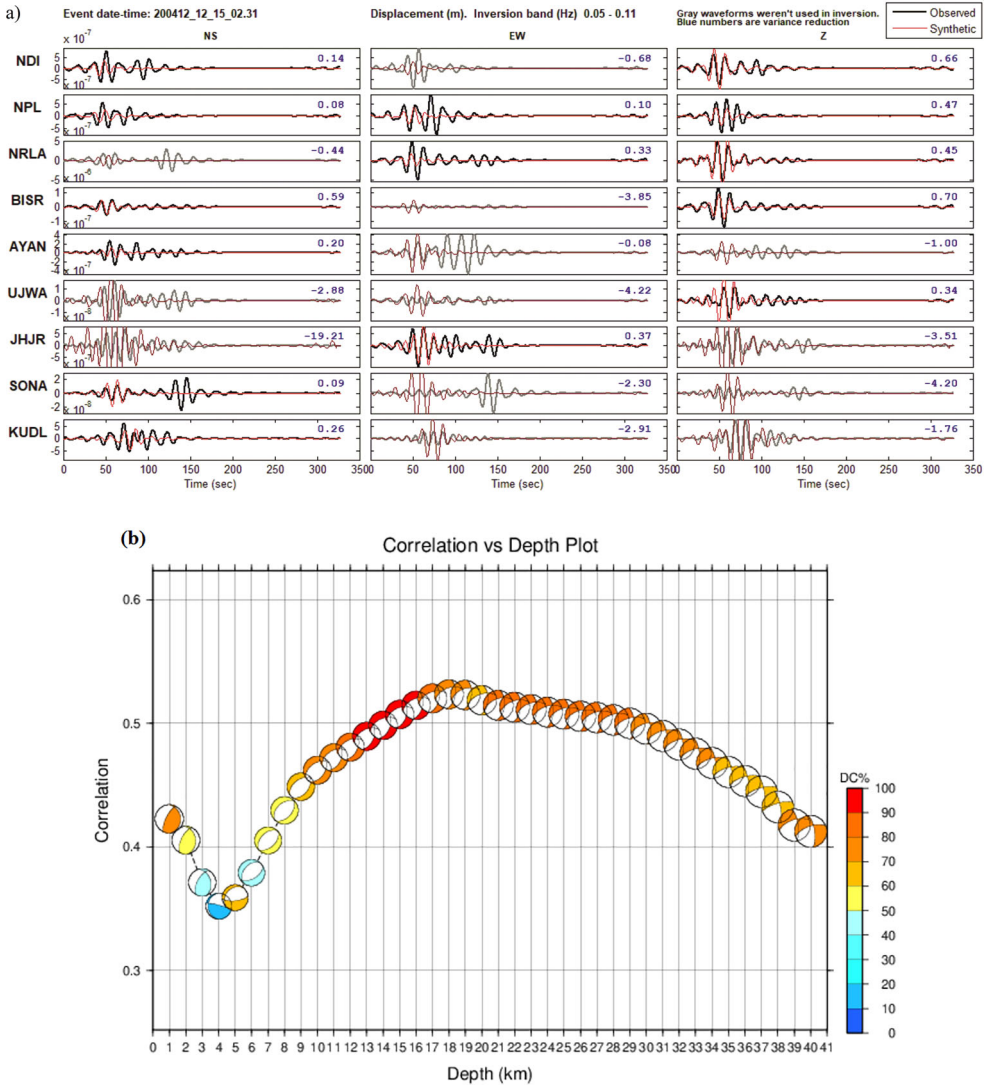


**Figure 3.** (a) Comparison of observed and synthetic waveforms of the mainshock using a centroid moment tensor inversion. Black and red waveforms represent the observed and synthetic waveforms, respectively. The observed waveforms in the light grey color indicate a negative correlation. A negative correlation means that one waveform is an upside-down version of the other waveforms. A poor correlation means that the two waveforms are not similar. The blue numbers represent the variance reduction between the waveforms. (b) Focal mechanism of the mainshock of the 12 April 2020 ( $M_L 3.5$ ) Delhi earthquake obtained at various trial depths by the vertical grid search method. The DC % of beach balls has been scaled on the right side.

in the region (Verma et al. 1995). We further suggest that the large number of past earthquakes along the major faults in and around the Delhi region might have stressed the lineaments in the epicentral region, and thus the mainshock might have reactivated the release of stored energy along such lineaments as small magnitude events. However, a detailed study is to be undertaken to understand the sources of these small magnitude



**Table 4.** Fault plane solution of the recent 12 April 2020 earthquake of Delhi region using moment tensor inversion.

S. N.	Date / Origin Time (IST)	Focal Depth (km)	Centroid Depth (km)	Nodal Plane 1			Nodal Plane 2			Mw
				Strike $\Phi$ 1	Dip $\delta$ 1	Rake $\lambda$ 1	Strike $\Phi$ 2	Dip $\delta$ 2	Rake $\lambda$ 2	
1	2020-04-12 17:45:02.3	16 ± 2.5	18	13 <sup>0</sup>	55 <sup>0</sup>	-135 <sup>0</sup>	253 <sup>0</sup>	55 <sup>0</sup>	-45 <sup>0</sup>	3.5

tremors in the region, which primarily may include precise estimation of focal mechanism and focal depths of these events (Dahal and Ebel 2020, 2019).

### 3.1.3. Source parameters

An analysis of the source parameters of the Delhi earthquakes ( $M_L$  3.5 and 2.7) using the S-wave recordings at the BBS stations, considering the Brune circular source model for the event (Brune 1970) were performed. The source parameters were obtained separate from the far-field displacement amplitude spectra of the S-waves on both the radial and transverse components. A sample displacement spectrum at the Thakurdwara (TKR) station is depicted in Figure 4. The spectra were corrected for geometrical spreading which decreased the amplitude of the signal with hypocentral distance. The quality factor is  $Q(f) = 253f^{0.80}$ , which was earlier estimated for the Himalayan arc region (Singh et al. 2004). The mean value of the source parameters of the recent earthquake, namely, the seismic moment, corner frequency, stress drop, and source radius, are estimated to be  $1.15 \times 10^{14}$  N-m, 5.7 Hz, 25.7 bars, and 300 m, respectively. The estimated result, therefore, is characterized  $\sim 26.0$  bars stress drop for the Delhi region, which is found to be within the stress drop range (10–144 bars) for stable-craton intraplate earthquakes (Kumar et al. 2014, Sairam et al. 2018). Further, the stress drop for the small to moderate earthquakes in the Central United States are found to be in the range of 46–300 bars, with a median of 84 bars (Huang et al. 2017). It is to mention that in general, higher stress drops usually coincide with the intraplate region (Sairam et al. 2018).

### 3.2. Strong ground motions

Strong-motion data from the 12 SMA stations for the Delhi tremors that occurred during 12 – 13 April 2020 were analyzed to understand ground-motion impact in terms of the peak ground acceleration (PGA), peak ground velocity (PGV) and peak ground displacement (PGD) at the recording stations. The stations were spread over the region at variable epicentral distances between 12 km to 104 km. The component-wise observed PGA, PGV, and PGD for the  $M_L$  3.5 and 2.7 events are listed in Tables 5 and 6, respectively. The  $M_L$  2.7 event being relatively a smaller event, the resulting strong ground motion recorded at only few stations and the maximum observed PGA were found to be quite feeble ( $< 0.6$  gals). A PGA decay curve with epicentral distance for  $M_L$  3.5 event is shown in Figure 5, which is found to be the best fit with a regression equation  $PGA_H = 472.89 * D^{-1.373}$ , where D is the epicentral distance. Evidently, the NDI station being located nearest to the event, with epicentral distance 12 km, shows the horizontal PGA to be 10.19 gals. Despite the site JMIU being located 25 Km away from the event, more than twice the distance of NDI, a slightly higher horizontal PGA 14.13 gals was

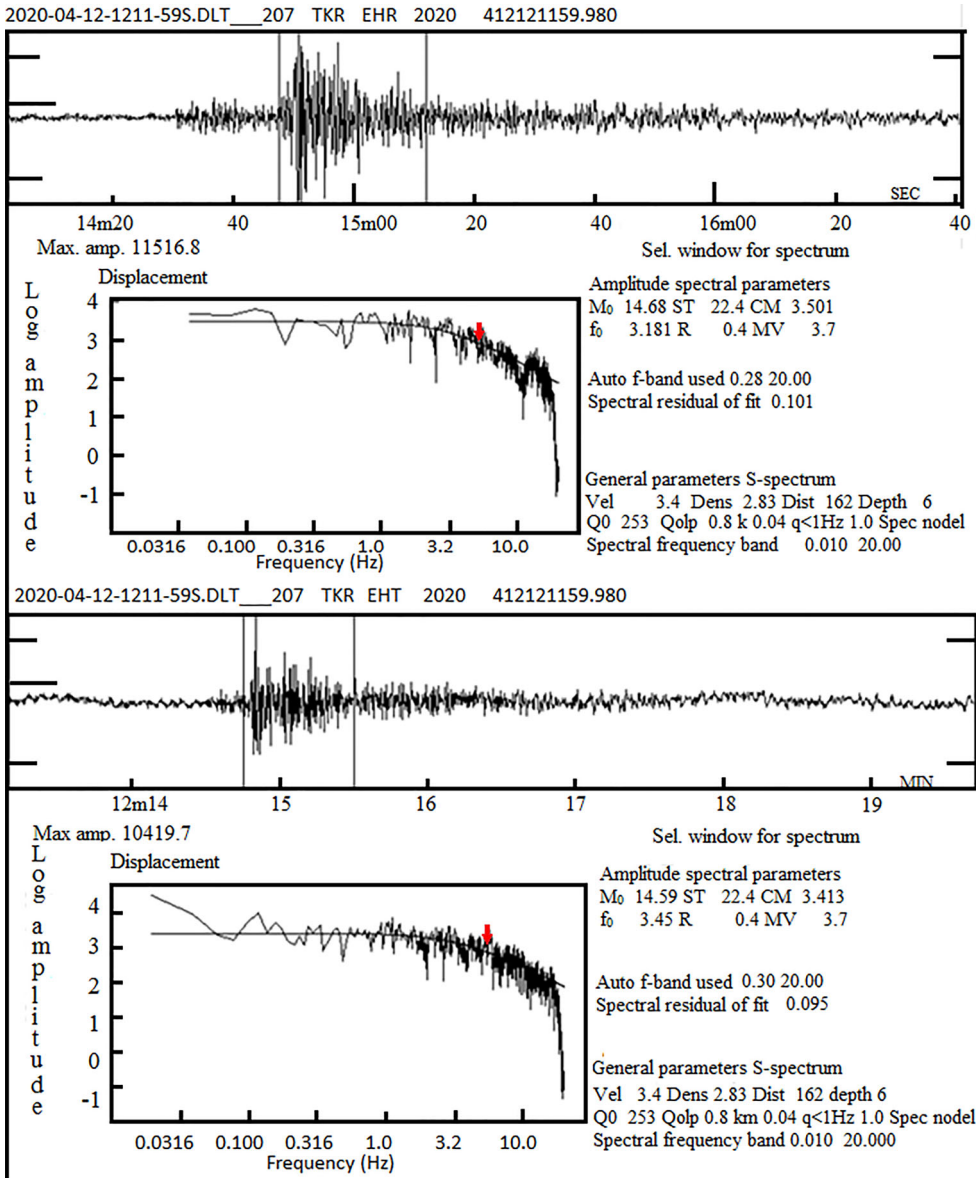


**Figure 4.** A typical example of a waveform and its amplitude spectrum for the earthquake of  $M_L 3.5$ , recorded at TKR BBS station. The waveform selected on the vertical displacement seismogram highlights the analyzed time window. The estimated amplitude spectral parameters such as amplitude and corner frequency from the waveform analysis are given adjacent to the spectra. Red arrows show the corner frequencies. The upper and lower panels correspond to radial and transverse components, respectively.

observed. Such higher ground motion at a relatively farther distance may be attributed to the local site effects. The JMIU station is established in an area underlain with a thick sediment column above the weathered basement rock (Shukla et al. 2007 and 2016). Although the PGA value at JMIU is the highest among all the sites, it was yet too feeble to result in damage in the area. We mention that  $PGA_H$  (Horizontal Peak Ground

**Table 5.** Strong motion parameters of  $M_L$  3.5 earthquake occurred on 12 April 2020.

S. N.	Station	Epicentral Distance (km) and Direction from the event	PGA (cm/s <sup>2</sup> = Gal)				PGV (cm/s)			PGD (cm)		
			V	NS	EW	$A_H^{\wedge}$	Z	N-S	E-W	Z	N-S	E-W
1.	NDI	12 / SSW	4.41	4.61	9.09	10.19	0.035	0.039	0.073	0.0015	0.0012	0.0026
2.	NRL	17 / NW	5.71	7.99	5.90	9.93	0.088	0.110	0.124	0.0038	0.0036	0.0050
3.	NPL	19 / SSW	7.13	9.30	7.43	11.90	0.118	0.111	0.107	0.0021	0.0030	0.0302
4.	LDR	22 / SSW	4.60	3.515	3.18	4.73	0.048	0.056	0.068	0.0020	0.0020	0.0270
5.	JMIU	25 / S	1.04	9.32	10.61	14.13	0.014	0.099	0.210	0.0092	0.0032	0.0684
6.	BIS	29 / SE	6.55	9.64	6.14	11.43	0.104	0.151	0.095	0.0018	0.0031	0.0023
7.	AYA	37 /SSW	1.03	1.12	1.87	2.18	0.015	0.015	0.025	0.0006	0.0007	0.0006
8.	UJW	43 / WSW	1.51	2.10	1.97	2.88	0.024	0.034	0.033	0.0007	0.0014	0.0013
9.	SON	63 / SSW	0.59	0.98	1.31	1.64	0.006	0.011	0.013	0.0004	0.0006	0.0005
10.	JHG	64 /W	1.12	2.15	1.66	2.72	0.015	0.028	0.026	0.0007	0.0011	0.0015
11.	PAL	76 / S	1.18	0.63	0.63	0.89	0.011	0.008	0.010	0.0004	0.0004	0.0005
12.	KUD	104 /SW	0.33	0.54	0.48	0.72	0.006	0.005	0.005	0.0007	0.0006	0.0030

Note:  $A_H^{\wedge}$  is the Horizontal Peak Ground Acceleration at the site [ $A_H^{\wedge} = \sqrt{(NS^2 + EW^2)}$ ].

**Table 6.** Strong motion parameters of  $M_w$  2.7 earthquake occurred on 13 April 2020.

S.N.	Stations	Epicentral Distance (km) / Direction from the event	PGA (cm/s <sup>2</sup> = Gal)				PGV (cm/s)			PGD (cm)		
			V	NS	EW	$A_H^{\wedge}$	Z	N-S	E-W	Z	N-S	E-W
1.	NDI	11 / SSW	0.84	0.97	0.92	0.97	0.0047	0.0048	0.0091	0.0004	0.0004	0.0004
2.	NPL	18 / SSW	0.56	0.60	0.57	0.595	0.0047	0.0058	0.0060	0.0019	0.0021	0.0023
3.	LDR	21 / S	0.28	0.17	0.15	0.174	0.0028	0.0021	0.0023	0.0016	0.0014	0.0012
4.	JMI	24 / S	0.12	0.16	0.14	0.158	0.0018	0.0000	0.0000	0.0006	0.0005	0.0006
5.	AYA	35 / SSW	0.08	0.08	0.11	0.083	0.0008	0.0007	0.0010	0.0005	0.0007	0.0005
6.	BIS	19 / SE	0.34	0.60	0.51	0.604	0.0039	0.0043	0.0038	0.0006	0.0004	0.0004
7.	SON	62 / SSW	0.05	0.06	0.07	0.058	0.0005	0.0005	0.0008	0.0004	0.0004	0.0004
8.	KUD	103 / SW	0.02	0.03	0.03	0.032	0.0005	0.0004	0.0005	0.0005	0.0004	0.0003

Acceleration) is estimated using the square root of the sum of the square of the PGA on the NS and EW components. Similarly, PGV and PGD are estimated for the events by integrating the acceleration waveform.

Felt reports of the ground shaking in the mainshock were received from people on the official website ([www.seismo.gov.in](http://www.seismo.gov.in)) and APP (RISEQ) of NCS, and have been tabulated in Table 7. A majority of the felt reports were equivalent to Intensity II on the Modified Mercalli intensity scale (MMI) scale (Figure 6). The two sites located at Rajendra Nagar and Lodhi Road reported relatively higher Intensity, viz., III and IV, respectively. However, the isoseismal map as estimated using a global empirical relationship (Hough 2012) depicts almost the entire NCT under the Intensity IV. Apparently, the entire region has experienced the ground shaking varying between intensity II - IV, which may be attributed to the local site effects (Shukla et al. 2016), types of buildings and construction practices.

### 3.3. Ambient noise

Ambient noise analyses of the continuously recorded ground motion data at NDI station (rock site) and UJWA station (soil site) for a 7-day period, prior to and during the prevailing lockdown condition due to unprecedented COVID-19 crisis, were

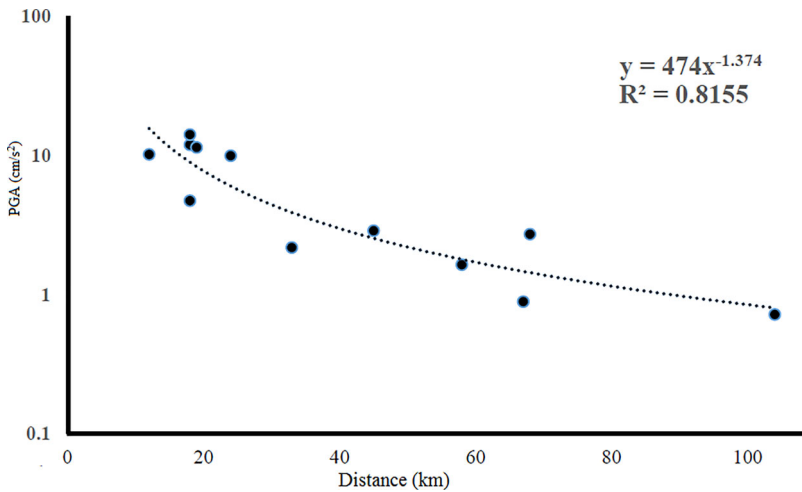


**Figure 5.** Decay plot of PGA variations with epicentral distance for the  $M_L3.5$  earthquake of 12 April 2020.

**Table 7.** MMI (Modified Mercalli Intensity) deduced from the Felt response received online for  $M_L3.5$  earthquake of 12 April 2020.

S. N.	MMI	Distance (km) / Direction from the event	Latitude ( $^{\circ}$ N)	Longitude ( $^{\circ}$ E)	Name of the Locality
1	II	17 / SW	28.669	77.159	New Rohtak Road
2	II	17 / SW	28.696	77.137	Kohat Enclave
3	II	18 / SSW	28.641	77.180	Rajendra Nagar
4	III	19 / SSW	28.644	77.163	Ranjeet Nagar
5	II	18 / S	28.693	77.125	Pitampura
6	II	24 / SW	28.632	77.100	Fateh Nagar
7	II	18 / S	28.627	77.296	Mandawali West
8	IV	22 / SSW	28.589	77.221	Lodhi Road
9	II	21 / S	28.595	77.296	Mayur Vihar Extension
10	II	23 / S	28.569	77.252	Nehru Nagar
11	II	26 / SSW	28.560	77.203	Green Park Extension
12	II	30 / SSW	28.542	77.142	Vasant Kunj
13	II	31 / SSW	28.525	77.149	Vasant Kunj
14	II	17 / ESE	28.702	77.421	Gaziabad Bypass

carried out. The power spectrum densities (PSD) of the background noise in both the segments were estimated using the PASCAL Quick Look Xtended (P.Q.L.X) package (McNamara and Boaz 2005). We considered only the Z component records in the analysis as representative of the ground motion to determine the noise power density acceleration spectrum and is measured in dB that is referred to 1  $((m/s^2)^2/Hz)$ . We mention that all the seismic stations were equipped with tri-axial broadband velocity sensors with 120 s period. The power density acceleration spectrum for both the segments (prior to and during the lockdown) at rock (NDI) and soil (UJWA) sites are shown in Figure 7. The Peterson Low Noise Model (LNM) and High Noise Model (HNM) are represented in the dark grey color. The noise spectra in both the segments are well constrained between the LNM and HNM in the case of the rock site (NDI); however, it crossed the HNM in the case of the soil site (UJWA) prior to the lockdown period, indicating it is a noisy site. It is important to mention that the

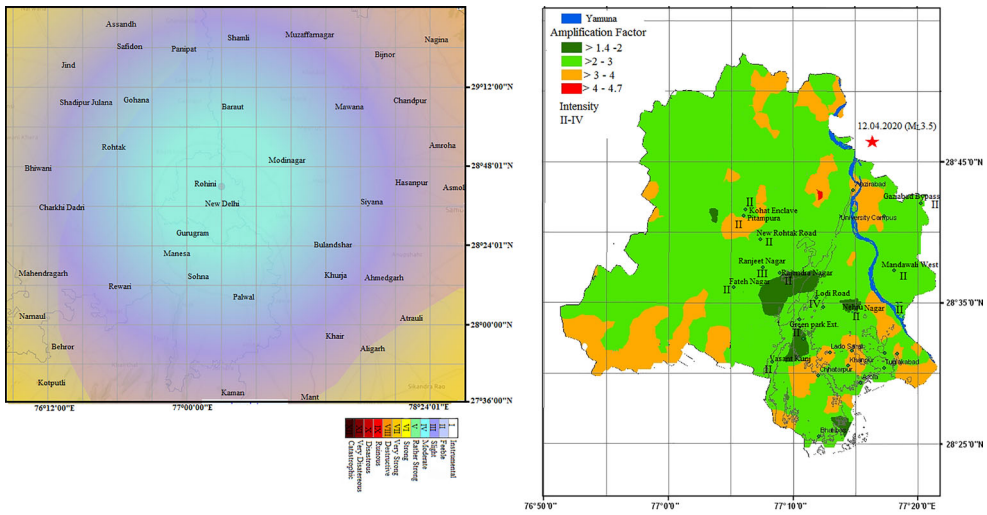


Figure 6. Left panel shows the Intensity map of earthquake of the  $M_L3.5$  earthquake occurred on 12 April 2020 using the empirical relation. The right panel shows the observed MMI Intensity based on the felt responses received online for the mainshock ( $M_L3.5$ ), which is overlaid on the amplification map of the NCT Delhi (Modified after Shukla et al. 2016). Intensity is depicted in Roman numerals. The star indicates the mainshock of 12 April 2020.

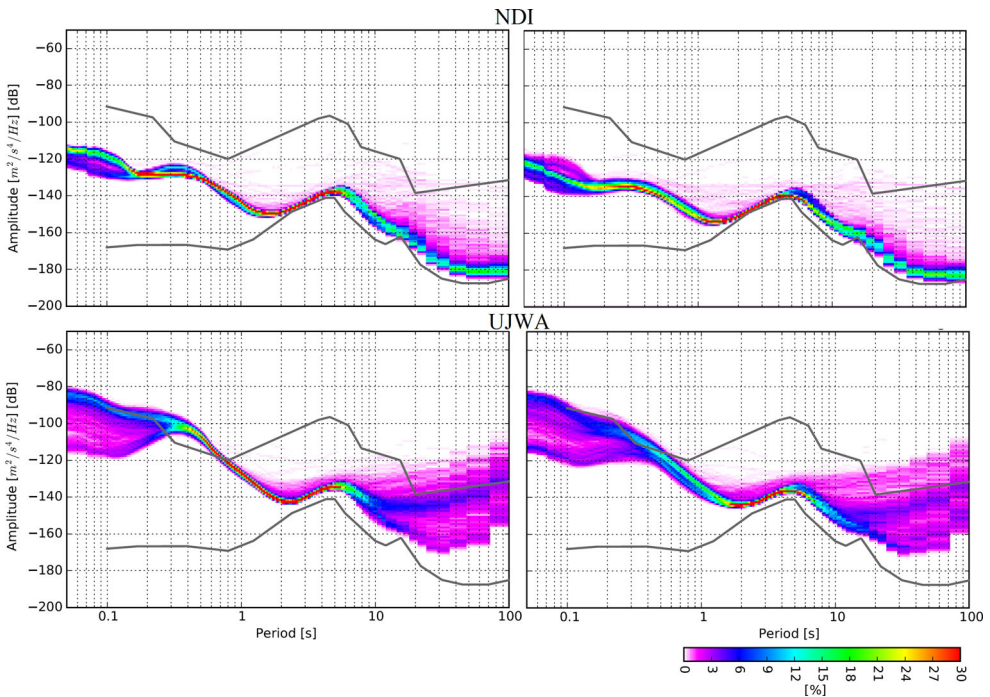


Figure 7. Comparison of the vertical component median seismic noise of the BBS stations at NDI and UJWA before (left panel) and during the lockdown (right panel) with high and low noise models of Peterson (1993). The power spectral densities (PSDs) are in units of dB with respect to acceleration. The color scale (%) represents the perturbation in the noise.

noise spectrum of the UJWA site during the lockdown period falls well within the upper bracket of the standard noise model i.e. HNM. At both the sites the ambient noise levels were higher than the LNM, but they also were found to be relatively stable as evidenced by the probabilities. Figure 7 shows about 10 dB decrease in the noise level at both the rock as well as soil sites during the lockdown period in the high-frequency range between 1 Hz to 10 Hz. However, a slight decrease in noise level at lower frequencies around 0.1 Hz is observed in both the cases. We mention that such long period signals are mostly related to in the quasi stationary state (Kumar et al. 2012), which is described as approximately time independent out of equilibrium state such as oceanic waves and wind etc. Further, a drop in average ground displacement from 25 nm to 8 nm indicates a better recording of the seismic signals during the lockdown period, even at relatively noisy sites located in the urban agglomerations.

#### 4. Conclusion

We have analyzed the broadband waveform and strong motion records of the April 2020 earthquakes, which shook the NCT Delhi and its surrounding regions. The epicenter of the event of 12 April 2020 ( $M_L$  3.5) was found to be located in the NCR close to the East district boundary of NCT Delhi. The aftershocks ( $M < 3.0$ ) that occurred during 12–16 April 2020 were primarily located to the SW of the mainshock. The focal mechanism of the mainshock is estimated using a moment-tensor inversion approach, which reveals normal faulting with a strike slip component. Although the nodal planes of the event did not coincide with any of the existing identified faults, they were found consistent with the NE - SW trending lineaments mapped in the region. The past events along the major faults in Delhi and surrounding regions might have stressed the lineaments in the epicentral area, which probably reactivated due to the mainshock of 12 April 2020 causing small magnitude events. However, we suggest a detailed analysis to be undertaken to understand the causative source of these small magnitude events that occurred after the mainshock. The amplitude spectra of the S-waves indicate the seismic moment of mainshock to be  $1.15 \times 10^{14}$  N-m. The stress drop during the event is observed close to the lower range of the stress drop (i.e.  $\sim 30$  bars) of the stable continental region in India. We emphasize that the event was felt widely probably due to the reduced mobility in Delhi and surrounding region. Due to the prevailing lockdown situation, the majority of the people were confined to their houses in Delhi and nearby areas where the buildings are mainly taller and are mostly erected over thick soil cover. Hence, the event could be felt by many people in the region. The strong ground motion analyses reveal a maximum peak ground acceleration (PGA) to be 14.13 gals at the JMIU site for the mainshock ( $M_L$  3.5) that was felt in the region with maximum intensity IV at Lodhi Road to the SW of the epicenter. However, for the aftershock on 13 April 2020 ( $M$  2.7) the maximum PGA was feeble ( $< 0.6$  gals) and hence it could not be felt widely. The noise analysis of the ground motion prior to and during the nationwide lockdown due to the unprecedented COVID-19 suggests a significant reduction of noise ( $\sim 10$  dB) at rock as well as soil sites in the frequency band 1–10 Hz during the

lockdown, which probably improved the ground motion seismic recording of the recent tremors of Delhi region. A clear peak of the P-wave in the mainshock record at the Latur seismic observatory, located about 1100 km away, indicates reduced noise level at the recording site. We attribute such clear recording of the phases at far distance to the silence caused due to country wide COVID-19 lockdown.

## Acknowledgments

The authors thank the Secretary, Ministry of Earth Sciences (MoES) New Delhi for all necessary support to carry out this research. We also sincerely thank the Editor-in-Chief and the anonymous reviewers for their constructive comments that improved the manuscript. The scientific and technical staffs of NCS, New Delhi are deeply acknowledged for maintaining the seismic stations and data. The NCS is highly acknowledged for the seismic waveform data for this study. A few figures were drawn using the freely available software GMT (Wessel and Smith 1998).

## Disclosure statement

No potential conflict of interest was reported by the author(s).

## References

- Bansal BK, Singh SK, Dharmaraju R, Pacheco JF, Ordaz M, Dattatrayam RS, Suresh G. 2009. Source study of two small earthquakes of Delhi, India, and estimation of ground motion from future moderate, local events. *J Seismol.* 13(1):89–105.
- Bansal BK, Verma M. 2012. The M 4.9 Delhi earthquake of 5 March 2012. *Curr Sci.* 102(12): 1704–1708.
- BIS: 1893 (Part 1). 2002. Indian standard criteria for earthquake resistant design of structures, Part 1 - general provisions and buildings. 5th ed. New Delhi: Bureau of Indian Standards; p. 42.
- Brune JN. 1970. Tectonic stress and spectra of seismic shear waves from earthquakes. *J Geophys Res.* 75(26):4997–5009.
- Chun K-Y. 1986. Crustal block of the western Ganga basin: a fragment of oceanic affinity? *Bull Seismol Soc Am* 76 (6):1687–1698.
- Dahal NR, Ebel JE. 2019. Method for determination of depths and moment magnitudes of small-magnitude local and regional earthquakes recorded by a sparse seismic network. *Bull Seismol Soc Am.* 109(1):124–137.
- Dahal NR, Ebel JE. 2020. Method for determination of focal mechanisms of magnitude 2.5–4.0 earthquakes recorded by a sparse regional seismic network. *Bull Seismol Soc Am.* 110(2): 715–726.
- GSI. 2000. Seismotectonic atlas of India and its environs. Kolkata: Geological Survey of India, Special Publication; p. 59.
- Gupta SK, Sharda YP. 1996. A geotechnical assessment of Delhi earthquake of July 28, 1994. *Proc Int Conf Dis Mitin, Madras.* 1: A1/26–A1/31.
- Havskov J, Ottemoller L. 1999. SeisAn Earthquake analysis software. *Seis Res Lett.* 70(5): 532–534.
- Hough SE. 2012. Initial assessment of the intensity distribution of the 2011 Mw 5.8 Mineral, Virginia, Earthquake. *Seismol Res Lett.* 83 (4):649–657.
- Huang Y, Ellsworth WL, Beroza GC. 2017. Stress drops of induced and tectonic earthquakes in the central United States are indistinguishable. *Sci Adv.* 3 (8):e1700772. <https://doi.org/10.1126/sciadv.1700772>.

- Hukku BM. 1966. Probable causes of earthquake in the Delhi- Sonipat area. Proc III Sysmp Earthquake Engg, Roorkee. pt. II:75–80.
- Iyengar RN. 1999. Earthquakes in ancient India. *Curr Sci.* 77(6):827–829.
- Kayal JR. 2001. Microearthquake activity in some parts of the Himalaya and the tectonic model. *Tectonophysics.* 339 (3–4):331–351.
- Kumar S, Chopra S, Choudhury P, Singh AP, Yadav RBS, Rastogi BK. 2012. Ambient noise levels in Gujarat State (India) seismic network. *Geomatics Nat Hazard Risk.* 3 (4):342–354.
- Kumar S, Kumar D, Rastogi BK. 2014. Source parameters and scaling relations for small earthquakes in the Kachchh region of Gujarat, India. *Nat Hazards.* 73(3):1269–1289.
- Kumar N, Sharma J, Arora BR, Mukhopadhyay S. 2009. Seismotectonic model of the Kangra–Chamba sector of Northwest Himalaya: constraints from joint hypocentre determination and focal mechanism. *Bull Seismol Soc Am.* 99(1):95–109.
- McNamara DE, Boaz RI. 2005. Seismic noise analysis using power spectral densities probability density function: A stand-alone software package. p. 29. U. S. Geol. Survey Open File Report, NO. 2005-1438, USGS, Reston, Virginia.
- Mitra S, Kainkaryam SM, Padhi A, Rai SS, Bhattacharya SN. 2011. The Himalayan foreland basin crust and upper mantle. *Phys Earth Planet Inter.* 184 (1–2):34–40.
- Sairam B, Singh AP, Kumar MR. 2018. Comparison of earthquake source characteristics in the Kachchh Rift Basin and Saurashtra horst, Deccan Volcanic Province, western India. *J Earth Syst Sci.* 127 (4):55..
- Shukla AK, Prakash R, Singh RK, Mishra PS, Bhatnagar AK. 2007. Seismotectonics implications of Delhi region through fault plane solutions of some recent earthquakes. *Curr Sci.* 93(12):1848–1853.
- Shukla AK, Singh RK, Mandal HS, Pandey AP, et al. 2016. A report on seismic microzonation of NCT Delhi on 1:10,000 scales. New Delhi: National Centre for Seismology, Ministry of Earth Sciences.
- Singh RP. 2020. Pandemic lockdown sensitizes New Delhi to earthquake risk. *Temblor*, <http://doi.org/10.32858/temblor.087>.
- Singh SK, Garcia D, Pacheco JF, Valenzuela R, Bansal BK, Dattatrayam RS. 2004. Q of the Indian Shield, *Bull. Seismo Soc Am.* 94(4):1564–1570.
- Singh SK, Kumar A, Suresh G, Ordaz M, Pacheco JF, Sharma ML, Bansal BK, Dattatrayam RS, Reinoso E. 2010. Delhi earthquake of 25 November 2007 (Mw 4.1): Implications for seismic hazard. *Curr Sci.* 99(7):939–947.
- Sokos E, Zahradnik J. 2008. ISOLA – A FORTRAN code and Matlab GUI to perform multiple point source inversion of seismic data. *Comput Geosci.* 34(8):967–977.
- Suresh G, Jain S, Bhattacharya SN. 2008. Lithosphere of Indus block in the northwestern Indian subcontinent through Genetic Algorithm inversion of surface-wave dispersion. *Bull Seismol Soc Am.* 98 (4):1750–1755.
- Tripathy-Lang A. 2020. Don't panic, prepare! Delhi earthquakes remind citizens of risk. *Temblor*. <http://doi.org/10.32858/temblor.096>.
- Verma RK, Roonwal GS, Kamble VP, Mohanty WK, Dutta U, Gupta Y, Chatterjee D, Kumar N, Chauhan PKS. 1995. Seismicity of Delhi and its surrounding region. *J. Himalayan Geol.* 6:75–82.
- Wessel P, Smith WHF. 1998. New, Improved Version of Generic Mapping Tools Released. *Eos Trans Agu.* 79(47):579–579. <http://dx.doi.org/10.1029/98EO00426>.